AN ULTRASONIC RESONATOR FOR DETERMINING SPEED OF SOUND AND ABSORPTION IN SMALL VOLUMES OF LIQUID MEDIA

BY

DAVID CONKLIN DENNEY

B.S., United States Naval Academy, 1966

THESIS

Submitted in partial fulfillment of the requirements
for the degree of Master of Science in Electrical Engineering
in the Graduate College of the
University of Illinois at Urbana-Champaign, 1972

Urbana, Illinois

ACKNOWLEDGMENTS

The author wishes to express his appreciation to his advisor, Professor Floyd Dunn, for suggesting the thesis problem and for his guidance throughout the study; to Mr. Steven Goss for his assistance during the initial work; and to Mr. Robert Noyes for constructing the device.

TABLE OF CONTENTS

I. INTRODUCTION

High intensity, noncavitating ultrasonic energy can produce unique changes in biological systems. The absorption of ultrasound in tissues appears to occur at the level of organization of biological macromolecules. However, the physical mechanisms responsible have not yet been elucidated.[1] Knowledge of the ultrasonic absorption coefficient and speed of sound in solutions of known materials as functions of frequency and temperature can aid in the identification of the particular mechanisms by which energy exchange processes occur.

The techniques for determining the absorption of ultrasound in liquid media fall into three basic categories, viz., pulse, continuous wave, and resonance methods. In one form of the pulse method, a short train of several sinusoidal waves travel a known distance through the specimen solution between an acoustic source and detector. The group velocity can be determined from knowledge of the time delay of the received signal after iniation of the pulse and the absorption is determined from the attenuated amplitude of the received signal. One form of the CW method is in an interferometer where the standing wave pattern is altered between the sound source and a reflecting surface by moving one of these structures relative to the other. The changes in acoustic impedance so produced can be observed as changes in the driving transducer current, which can be measured, and from which the sound velocity and absorption can be determined.[2]

The various methods available for determining the acoustic propagation properties of liquids were devised with little or no consideration

for the volume of material available for the measurement procedure. Further, it is characteristic that for lower frequencies, greater volumes are generally required in order to avoid effects due to diffraction phenomena. The necessity for having such large volumes available becomes a serious problem when biological macromolecules are to be treated in solutions, since only a few ca- be extracted for volumes of the order of liters (10 percent solutions) within the bounds of reasonable economics.

The resonance technique offers a method utilizing volumes less than 40 ml of specimen fluid. The purpose of this study was to investigate a resonator requiring 18 ml of fluid for velocity and absorption measurements. The device, a two piezoelectric transducer, variable frequency, fixed path interferometer has been described in detail by Eggers.[3]

The thesis comprises six sections:

1. The theoretical principles behind the operation of the interferometer;
2. Description of the mechanical and electrical details and of the associated instrumentation;
3. The measurement method;
4. A discussion of the degree to which the desired goals have been achieved;
5. A discussion of errors in the measurement procedure; and
6. Conclusions and thoughts for future study in order to improve the present model.

The unit was first studied using distilled water as the liquid under study. The velocity and absorption data for water compares favorably

with accepted values. Measurements made with a polyethylene glycol solution showed appreciable agreement with accepted values of velocity, i.e., within 0.5 percent. The absorption measurements were somewhat disappointing, deviating by as much as 70 percent from accepted values. The reasons for this discrepancy are not understood at present, but believed to be associated with mechanical design features of the cell.

II. THEORY OF THE RESONATOR

A. Resonant Frequencies of the System

The measuring cell is basically a fixed path two crystal acoustic interferometer. The magnitude of the absorption per wavelength ($\alpha\lambda$) is dependent on the quality factor (Q) of the device, and the Q is obtained from bandwidth measurements. The velocity of sound in the specimen liquid being tested is related to the frequency difference between adjacent resonant peaks.

The cell, shown schematically in Fig. 1, consists of two piezoelectric quartz transducers, Q_1 and Q_2, closely matched in frequency, of thickness, d, and diameter, D, and separated by a distance, l. The cylindrical cavity between the two quartz crystal discs is occupied by the specimen liquid under study.

At resonance of the cavity, the standing wave pattern is either in the symmetrical mode or in the asymmetrical mode, i.e., $\pi/2$ radians out of phase. The two resonant modes are shown in Fig. 2. An alternative way of stating this condition is to say that the sending crystal, Q_1, at resonance radiates into an acoustic impedance magnitude, at the plane S, of zero or infinity. At resonance, then, relations may be developed considering the left half of the system up to the plane S and is shown in Fig. 3, where

Z_{Q0} = Acoustic impedance looking at the left face of crystal Q_1

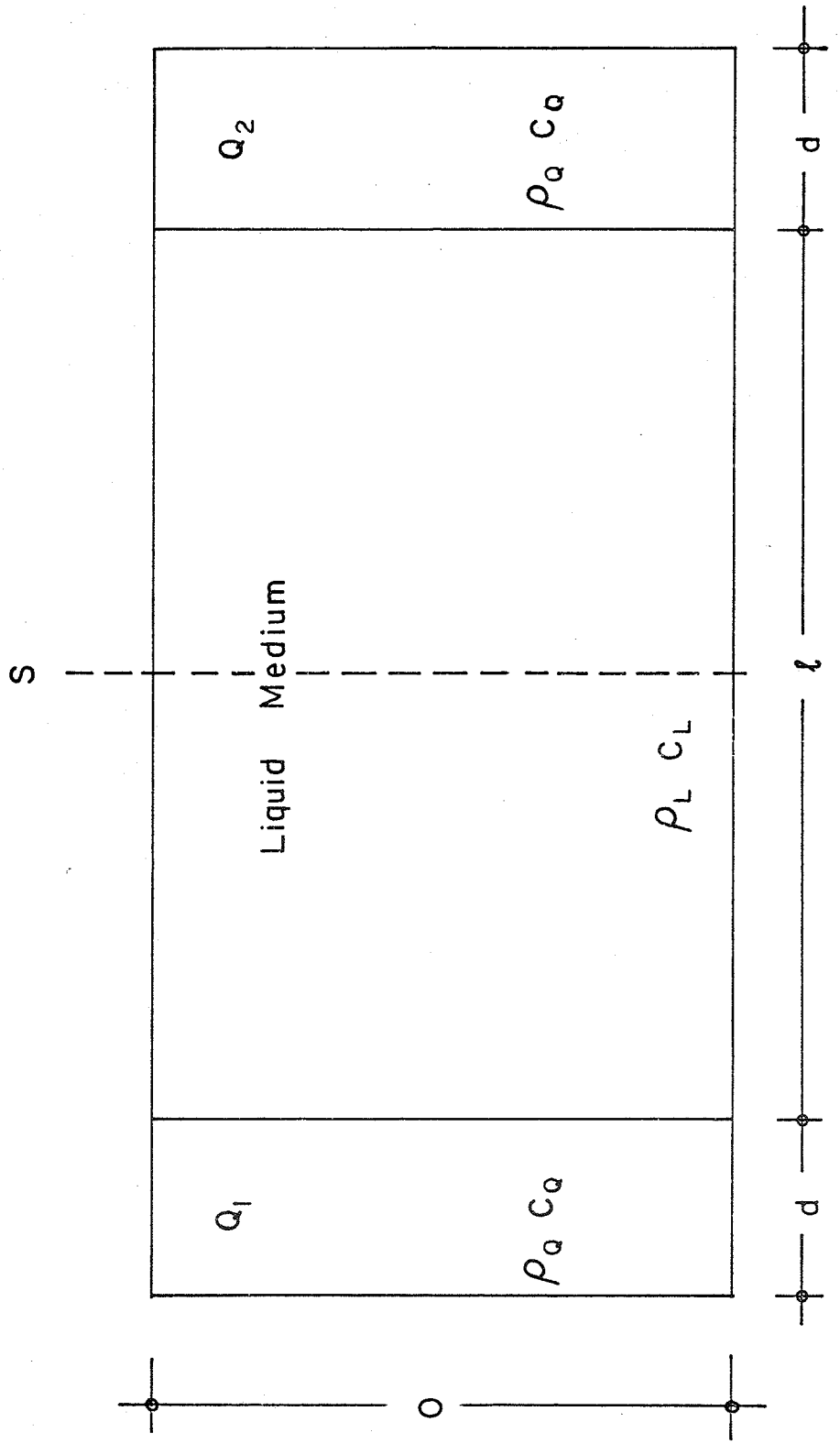

Figure 1 The Acoustic Cell

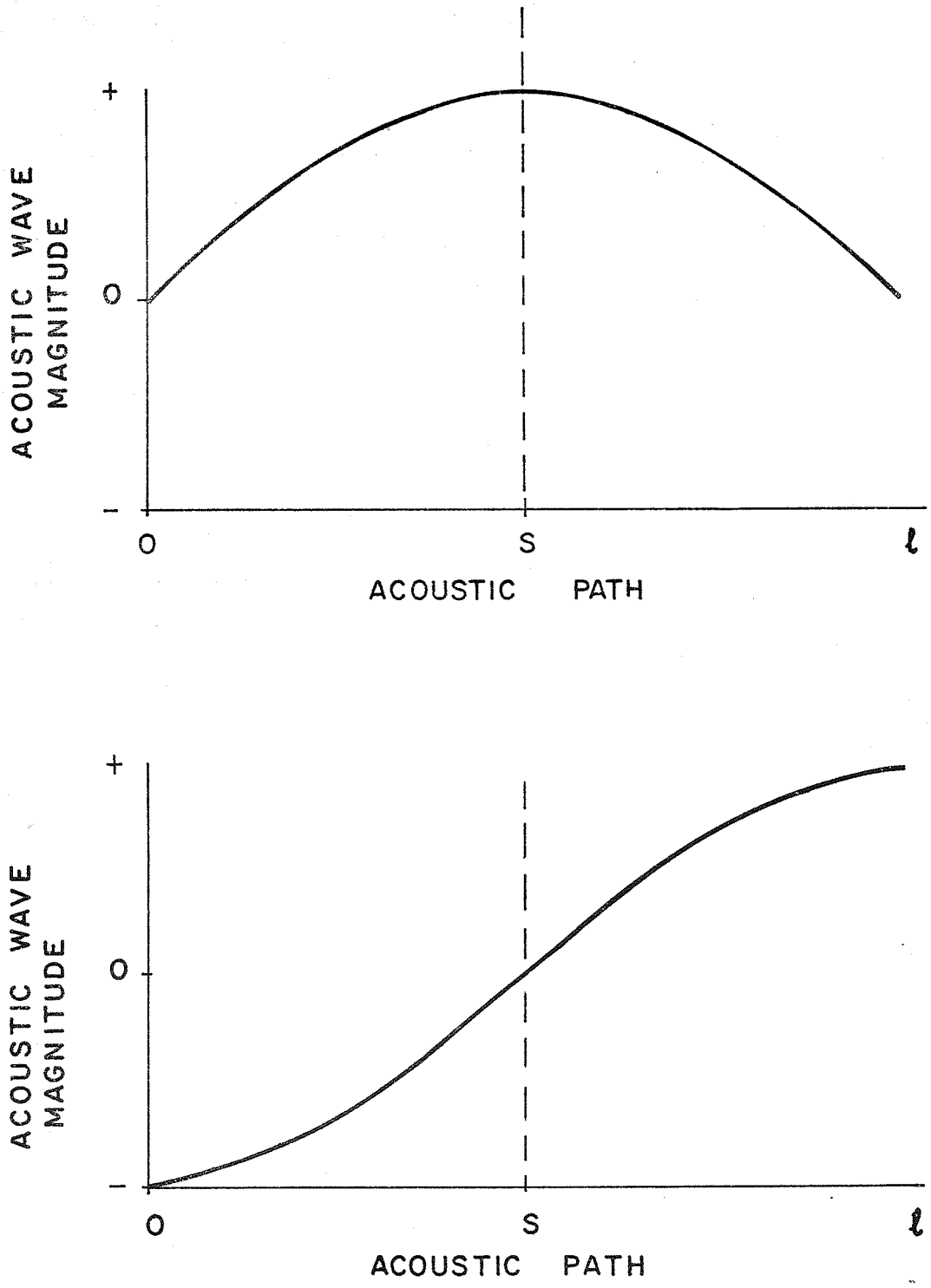

Figure 2 Symmetrical and Asymmetrical Modes

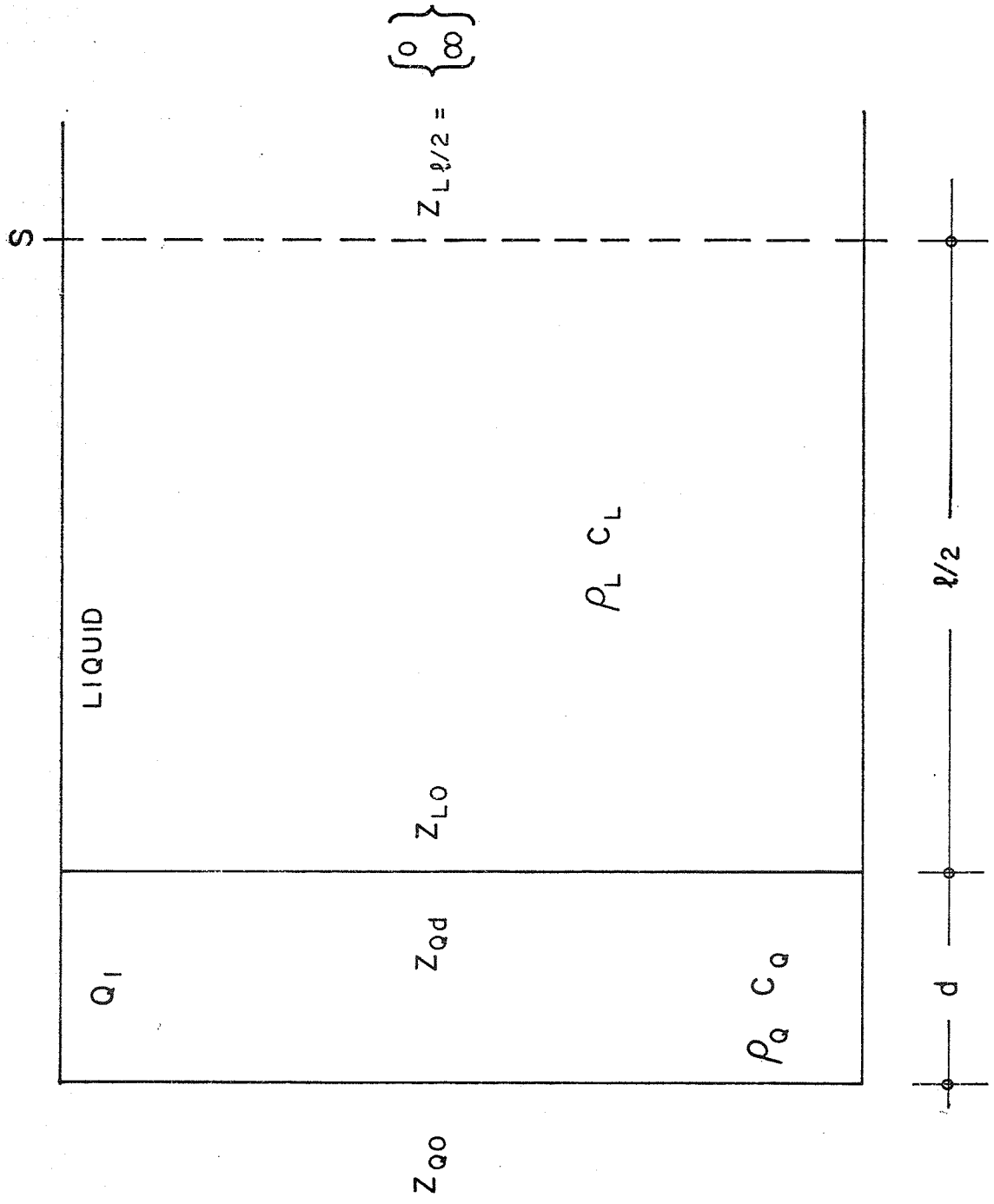

Figure 3 The Resonant System

Z_{LO} = Acoustic impedance looking at the left face of the liquid media

Z_{Qd} = Acoustic impedance at the right face of crystal Q_1

$Z_{L\ell/2}$ = Acoustic impedance at the plane S

$\rho_Q C_Q$ = Characteristic acoustic impedance of crystal Q_1

$\rho_L C_L$ = Characteristic acoustic impedance of the liquid

First, the acoustic pressure waves within the crystal will be examined. Figure 4 is an expanded view of crystal Q_1 shown in Fig. 3.

The incident and reflected sound pressure waves are p_i and p_r, respectively, at any point x. The equations for these waves are

$$p_i = Ae^{j(\omega t - kx)} \tag{1}$$

$$p_r = Be^{j(\omega t + kx)} \tag{2}$$

where

A = complex pressure amplitude

B = complex pressure amplitude

ω = angular frequency

k = wavelength constant = $2\pi/\lambda$

t = time

x = longitudinal position

The volume velocities of fluid flow corresponding to these two waves are given, respectively, by

$$V_i = p_i/\rho_Q C_Q/a \tag{3}$$

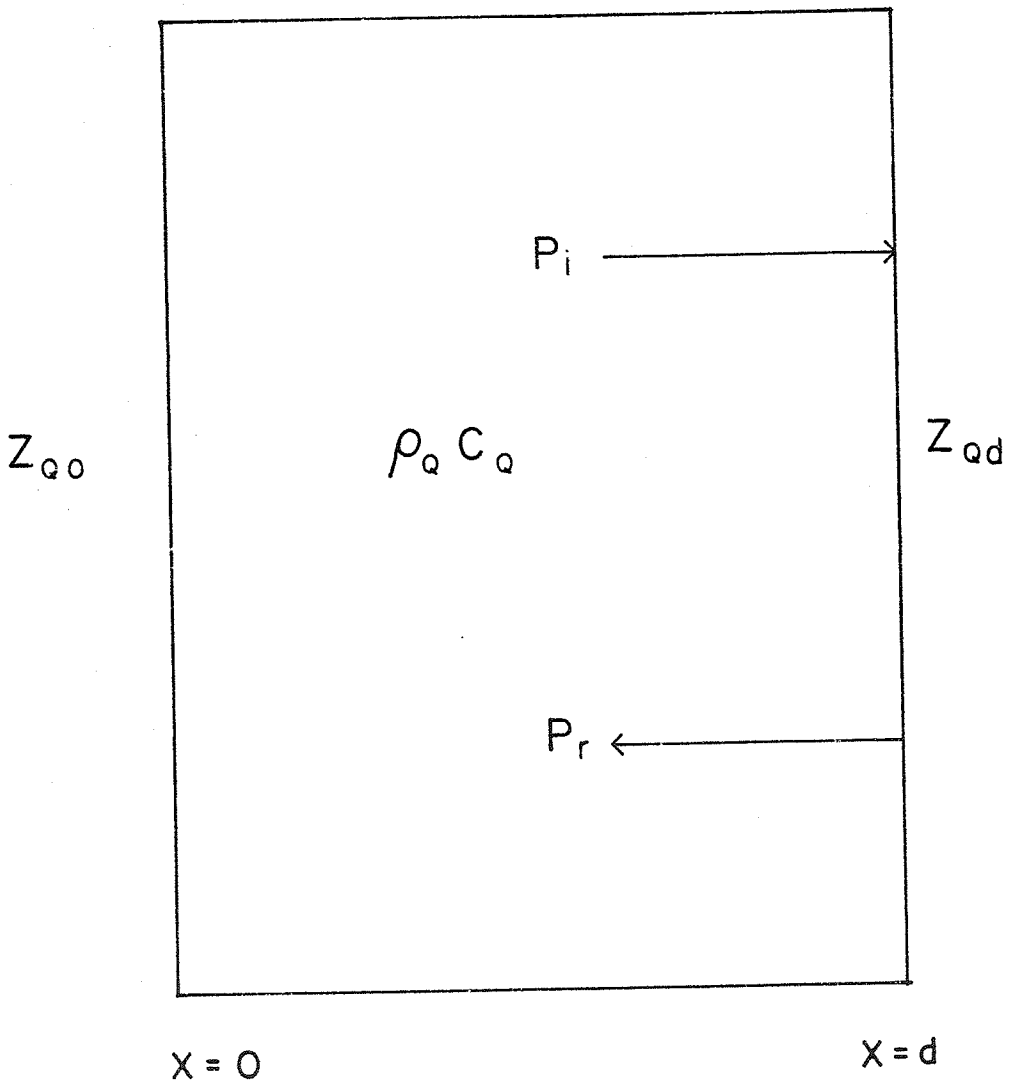

Figure 4 Crystal Q_1

$$V_r = -p_r/\rho_Q C_Q/a \tag{4}$$

where a is the surface area of the transducer. Because a standing wave exists within the cylinder, the acoustic impedance varies longitudinally from point to point.[4]

The acoustic impedance in the crystal is

$$\frac{p}{V} = Z = \frac{p_i + p_r}{V_i + V_r} = \frac{\rho_Q C_Q}{a} \cdot \frac{p_i + p_r}{p_i - p_r} \tag{5}$$

or

$$Z = \frac{\rho_Q C_Q}{a} \cdot \frac{Ae^{j(\omega t-kx)} + Be^{j(\omega t+kx)}}{Ae^{j(\omega t-kx)} - Be^{j(\omega t+kx)}} \tag{6}$$

and, finally,

$$Z = \frac{\rho_Q C_Q}{a} \cdot \frac{Ae^{-jkx} + Be^{jkx}}{Ae^{-jkx} - Be^{jkx}} \tag{7}$$

Two positions of interest are x = 0, the left surface of the crystal which, in this case, is exposed to air, and at x = d, the right surface of the crystal which drives the fluid column.

$$Z_{Q0} = \frac{\rho_Q C_Q}{a} \cdot \frac{A + B}{A - B} \tag{8}$$

$$Z_{Qd} = \frac{\rho_Q C_Q}{a} \cdot \frac{Ae^{jkd} - Be^{jkd}}{Ae^{-jkd} - Be^{jkd}} \tag{9}$$

Equations 8 and 9 are used to form a new expression which is independent of the complex pressure amplitudes A and B. Taking the ratio of A to B from Eq. 8 yields

$$\frac{A}{B} = \frac{Z_{Q0} + \rho_Q C_Q/a}{Z_{Qd} - \rho_Q C_Q/a} \tag{10}$$

Similarly, from Eq. 9 gives

$$\frac{A}{B} = \frac{Z_{Qd} + (\rho_Q C_Q/a)e^{2jkd}}{Z_{Qd} - (\rho_Q C_Q/a)} \tag{11}$$

Equating 10 and 11 and solving for Z_{Q0},

$$Z_{Q0} = \frac{\rho_Q C_Q}{a} \cdot \frac{Z_{Qd} + j(\rho_Q C_Q/a) \tan kd}{(\rho_Q C_Q/a) + jZ_{Qd} \tan kd} \tag{12}$$

In the actual situation, the medium facing the left surface of the crystal is air, which has a very small characteristic impedance compared with that for quartz, such that $Z_{Q0} = 0$ to a degree of error less than 0.1 percent. Equation 12, therefore, simplifies to

$$Z_{Qd} = -\frac{j\rho_Q C_Q}{a} \tan kd \tag{13}$$

Figure 5 illustrates the similar analysis for the liquid. Thus,

$$Z_{L0} = \frac{\rho_L C_L}{a} \cdot \frac{Z_{L\ell/2} + j(\rho_L C_L/a) \tan k\,\ell/2}{j(Z_{L\ell/2}) \tan k\,\ell/2 + (\rho_L C_L/a)} \tag{14}$$

The points x = d in the crystal and the point x = 0 in the fluid column are the same positions in the cell. The boundary conditions of continuity of pressure and volume velocity may be replaced by a condition of continuity of their ratio, i.e., continuity of acoustic impedance. Therefore, equating Z_{Qd} and Z_{L0} yields

$$\frac{-j\rho_Q C_Q}{a} \tan kd = \frac{\rho_L C_L}{a} \cdot \frac{Z_{L\ell/2} + j(\rho_L C_L/a) \tan k\,\ell/2}{(\rho_L C_L/a) + jZ_{L\ell/2} \tan k\,\ell/2} \tag{15}$$

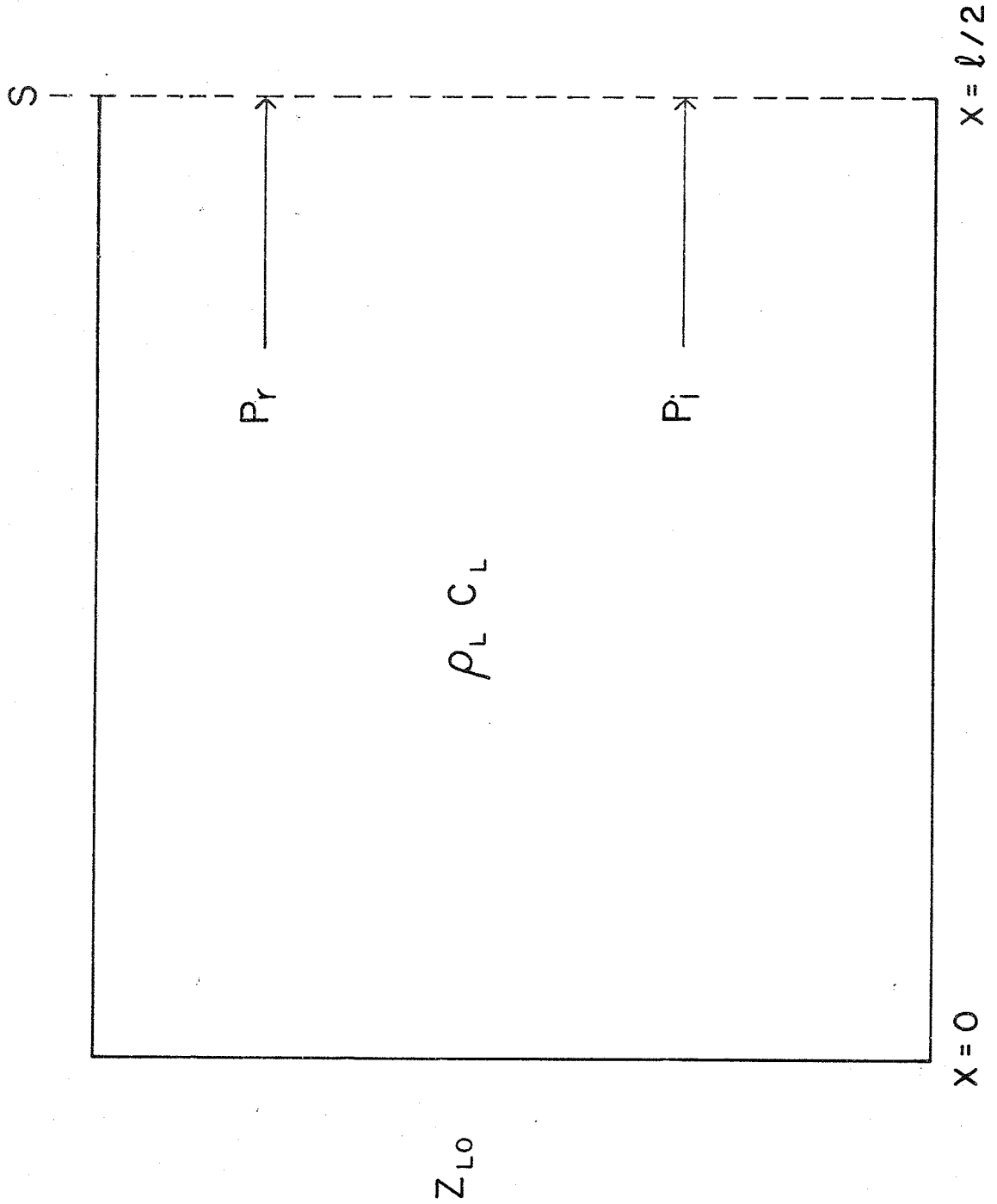

Figure 5 The Fluid Column

At resonance, the impedance of the liquid at $x = \ell/2$ is either zero or infinity, depending on the phase relation of the incident and reflected waves.

For $Z_{L\,\ell/2} = 0$, Eq. 15 becomes

$$\rho_Q C_Q \tan kd = - \rho_L C_L \tan k\,\ell/2 \tag{16}$$

And for $Z_{L\,\ell/2}$ = infinity yields

$$\rho_Q C_Q \tan kd = \rho_L C_L \operatorname{cotan} k\,\ell/2 \tag{17}$$

Therefore, depending on the phase relationship between the incident and reflected waves

$$\rho_Q C_Q \tan kd = \rho_L C_L \begin{bmatrix} -\tan \\ \operatorname{cotan} \end{bmatrix} k\,\ell/2 \tag{18}$$

We are interested in the behavior of the system at resonance and, since the measurements for absorption and velocity involve frequency measurements, it is desirable to express Eq. 18 in terms of the operating or resonant frequency, f_n, instead of the wave number and distance coordinate, kd.

The fundamental resonance frequency for the x-cut quartz crystal plate is

$$f_Q = \frac{C_Q}{2d} \tag{19}$$

Similarly, the fundamental resonance frequency of the liquid column containing an integral number of half-wavelengths is

$$f_L = \frac{C_L}{2\ell} \tag{20}$$

where C_Q and C_L are the velocities of sound in quartz and the liquid media, respectively. Noting that at a resonant frequency $k_n = \frac{\omega_n}{C} = \frac{2\pi f_n}{C}$ and utilizing Eqs. 19 and 20, then

$$kd = \frac{2\pi f_n d}{C_Q} = \frac{\pi f_n}{f_Q} \tag{21}$$

and

$$k\,\ell/2 = \frac{2\pi f_n}{C_L 2} = \frac{\pi f_n}{2 f_L} \tag{22}$$

Substituting Eqs. 21 and 22 into Eq. 18 yields

$$\rho_Q C_Q \tan\left(\frac{\pi f_n}{f_Q}\right) = \rho_L C_L \begin{bmatrix}-\tan \\ \text{cotan}\end{bmatrix} \left(\frac{\pi}{2}\frac{f_n}{f_L}\right) \tag{23}$$

Transducer Q_1 is driven by a sinusoidal voltage and produces resonances in the liquid medium at particular frequencies f_n that obey Eq. 23, the transcendental resonance equation.[3]

B. Velocity Measurement

The velocity of sound in the specimen fluid is determined with the interferometer from knowledge of the separation distance between the transmitter and receiver crystals and the frequency difference between adjacent resonant frequencies of the cell. Figure 6 shows two standing wave patterns of adjacent resonances. At resonance, at $x = 0$ and $x = \ell$, an integral number of half-wavelengths within the fixed distance ℓ occurs.

Thus, letting m be any integer,

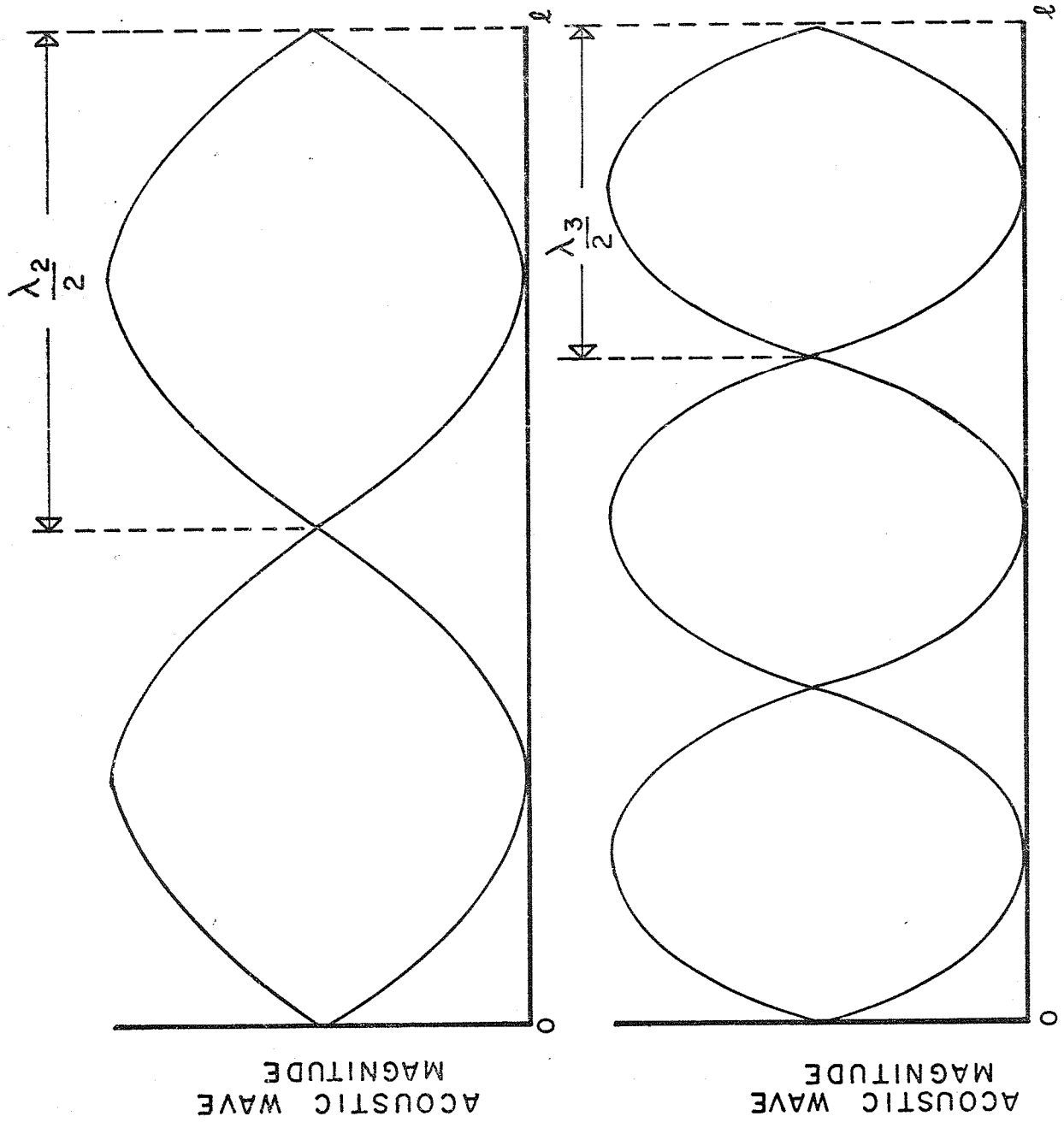

Figure 6 Two Adjacent Standing Wave Patterns

$$\ell = \frac{m\lambda_m}{2} \tag{24}$$

and

$$\lambda_m = \frac{C}{f_m} \tag{25}$$

So

$$\ell = \frac{mC}{2f_m} = \frac{(m+1)}{2}\frac{C}{f_{m+1}} \tag{26}$$

and

$$f_{m+1} - f_m = \frac{(m+1)\ C - mC}{2\ell} \tag{27}$$

Finally

$$C = 2\ell\ [f_{m+1} - f_m] \tag{28}$$

Acoustic velocity may be determined by measuring the fixed acoustic path length of the interferometer, noting the frequency difference between adjacent resonant peaks and applying Eq. 28.

C. Absorption Measurement

The Q or quality of a resonating system is defined[3] as

$$Q = \frac{f_n}{\Delta f} = \frac{2\pi \text{ stored energy}}{\text{energy dissipated per cycle}} \tag{29}$$

where

f_n = the frequency at resonance

Δf = the frequency difference between the lower and upper half power frequencies

The amplitude of a plane progressive, sinusoidal wave decays exponentially as it propagates through a lossy, homogeneous unbounded medium according to

$$p(x) = p(o)e^{-\alpha x} \tag{30}$$

where

$p(x)$ = sound pressure amplitude at the point x in the field

$p(o)$ = initial pressure amplitude at point x = 0

α = absorption coefficient

The acoustic energy transported per unit area per unit time is given by the acoustic intensity as[4]

$$I = \frac{p^2}{2\rho C} \tag{31}$$

The intensity at x = 0 is

$$I(o) = \frac{p(o)^2}{2\rho C} \tag{32}$$

The intensity at a distance λ is

$$I(\lambda) = \frac{p(o)^2 e^{-2\alpha\lambda}}{2\rho C} \tag{33}$$

Since intensity is power per unit area and the cross-sectional area is a constant, the stored energy and the energy dissipated per cycle terms in Eq. 29 can be expressed in terms of the intensity as $I(o)$ and $I(o) - I(\lambda)$, respectively.

$$Q = \frac{2\pi\, I(o)}{I(o) - I(\lambda)} = \frac{2\pi\, p(o)^2/2\rho C}{p(o)^2/2\rho C - p(o)^2 e^{-2\alpha\lambda}/2\rho C} \tag{34}$$

and

$$Q = \frac{2\pi}{1 - e^{-2\alpha\lambda}} \tag{35}$$

Expanding,

$$e^{-2\alpha\lambda} = 1 - 2\alpha\lambda + \frac{(2\alpha\lambda)^2}{2!} \quad . \; . \; . \; .$$

For frequencies in the low megahertz region, where wave lengths are the order of 10^{-1}cm, and for absorption values of the order of 10^{-1} cm^{-1}, the first two terms of the series approximate the series to about 0.1 percent error. The expression for Q becomes

$$Q = \frac{2\pi}{1 - (1-2\alpha\lambda)} = \frac{\pi}{\alpha\lambda} \tag{36}$$

Referring to Eq. 29, we now have[3]

$$Q = \frac{f}{\Delta f} = \frac{\pi}{\alpha\lambda} \tag{37}$$

Equation 37 relates the bandwidth of a resonant peak to the absorption per wavelength ($\alpha\lambda$) at a resonant frequency of the cell.

The energy loss of the standing wave sound field in the cell is caused not only by absorption in the liquid specimen, but possibly also by additional losses from imperfect reflection at the transducer, wall friction losses, and acoustical beam spreading.

For the case where the specimen fluid is a solution, absorption has two components, that due to the dissolved chemical species and that due to the solvent. When the two absorption components can be assumed to add arithmetically, the absorption of the solute is determined from relation:[3]

$$\frac{1}{Q_{total}} = \frac{1}{Q_{solvent}} + \frac{1}{Q_{solute}} \tag{38}$$

Equation 38 yields, in analogy to Eq. 37

$$Q_{solute} = \frac{\pi}{\alpha\lambda_{solute}} = \frac{f}{\Delta f_{specimen} - \Delta f_{solvent}} \tag{39}$$

One important aspect of Eq. 39 is that the additional mechanical losses, described above, common to the bandwidths of both the solute and the solvent, are eliminated when the difference is formed.

III. DISCUSSION OF THE MEASUREMENT SYSTEM

A. Cell Description

Figure 7 is a full scale cross-sectional view of the interferometer constructed for this study. The cell, which rests in a wooden cradle, consists of four major brass sections and is shown assembled. Section I supports three adjustment screws, A_1, which control the alignment of the left crystal, Q_1, and houses the BNC connector, B_1. The resonant cavity, M, is formed when the two crystals are in place on the section II. The cavity is filled via the loading tube, L, which has a wing gate valve attached. An exhalation hole, E, in the top of the cell facilitates filling. A fluid conducting jacket, T, used for temperature control, surrounds section II. The right hand crystal, Q_2, is aligned by the adjustment screws, A_2, mounted in section III. Both crystals are mounted in brass rings, R_1 and R_2, and each ring is retained against a rubber gasket, D_2, by pressure from the adjustment screws. The gaskets were installed with a thin coating of vaseline on all sides to prevent leakage of the specimen fluid. Section IV houses the BNC connector, B_2.

The three adjustment screws, A_1, were chosen as size 3/8-64 since the larger number of threads per unit were found to be more useful for aligning the transducers, i.e., they provided appropriate sensitivity in the adjustment. The right hand screws, A_2, are 8-32 and are employed for initial positioning, i.e., they do not have to provide high sensitivity for alignment.

An initial problem associated with the alignment procedure was

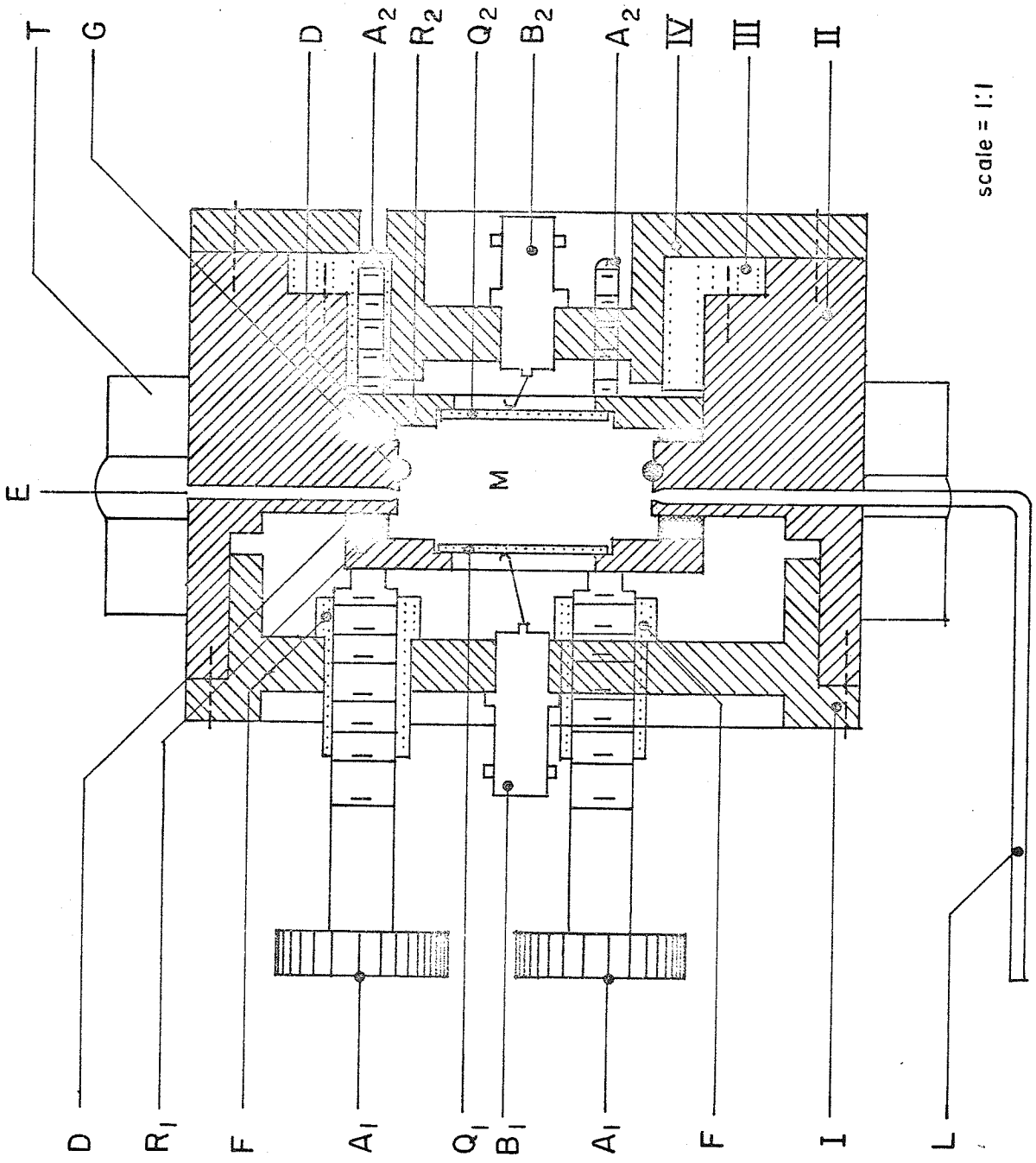

Figure 7 Cross Section of the Resonator

that lateral displacements of the screws resulted in displacements transmitted to the brass ring and crystal. The problem was circumvented by threading the screws through flanges F, which provided tighter bearing surfaces and stabilized the screws.

The cavity contains a rubber O-ring, G, which extends in the cell 0.0625 in. and, according to an earlier study,[3] produces a clean and even wave propagation, thereby increasing the Q. Rings extending into the cell greater distances (0.3 in.) were found to have adverse effects upon the Q.

General Electric Silicone Seal was used to mount the quartz crystals into the retaining rings. Upon curing, the silicone rubber formed a resiliant bond which did not load the crystals. The uncured adhesive was applied to the edge of the crystal with a syringe, and the transducer was then placed on the lip of the brass ring and centered with a cylindrical shell. This method of assembly provides for

1. Versatile adjustments of parallelism of the transducers,
2. A positive pressure seal at the silicone rubber joint by utilizing pressure of the fluid in the cell and thereby avoid leaking, and
3. An easily performed procedure for changing transducer sets having different fundamental resonant frequencies.

B. Temperature Control

Figure 8 is a diagram of the temperature control system which employs a reservoir of about ten gallons of water. Refrigeration and

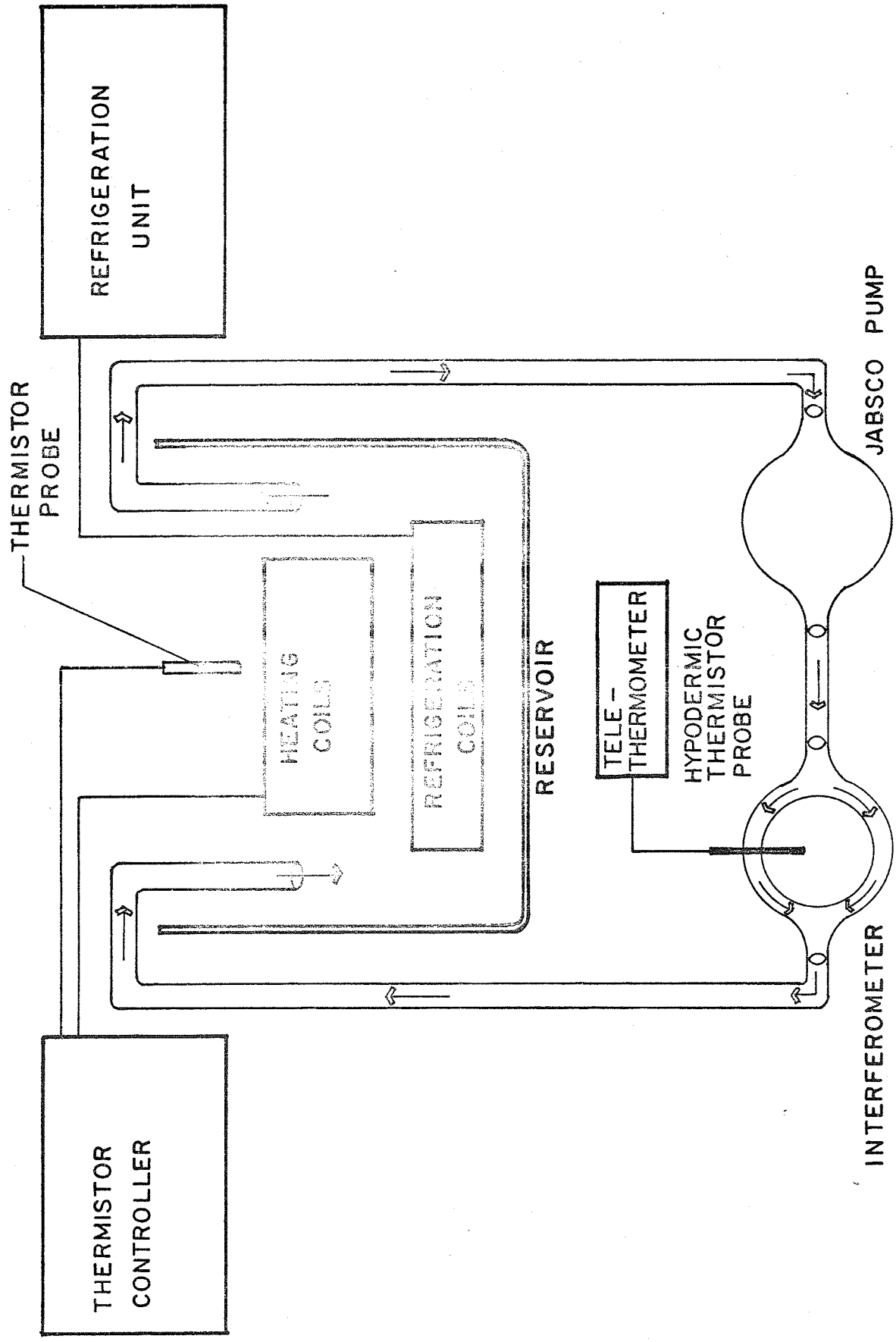

Figure 8 Temperature Control System

heating coils are provided to maintain the reservoir temperature. The heating coils are driven by a YSI model 72 proportional temperature controller which uses a liquid immersion thermistor probe to sense the temperature of the reservoir. The controller may be set to within 0.01°C and responds to variations of 0.005°C. Water of constant temperature is pumped from the bath, using a Jabsco pump model B3M6318, through plastic tubing and into the input nozzle of the temperature jacket surrounding the cell.

A calibrated YSI 22 gage hypodermic thermistor probe is inserted into the small air exit hole in the upper wall of the cell, and the temperature within the cell is then obtained with a Tele-thermometer. When operating within 3.0°C of room temperature, a twenty minute delay occurs from start-up time until the cell reaches temperature stability. As an example of the temperature stability obtained, no observable (0.1°C) variation occurs in the cell over a two hour period, when the external cell temperature (room temperature) varies 2.0°C.

Once temperature stability is reached, the probe is removed from the cell and inserted periodically for monitoring. Removal of the probe from the cell is necessary during acoustic positioning of the unit since it disturbs the sound field distribution in the cell.

C. Electrical System

Figure 9 shows the electrical assembly detail of the cell. The quartz transducers are gold plated on each major face, and each is grounded

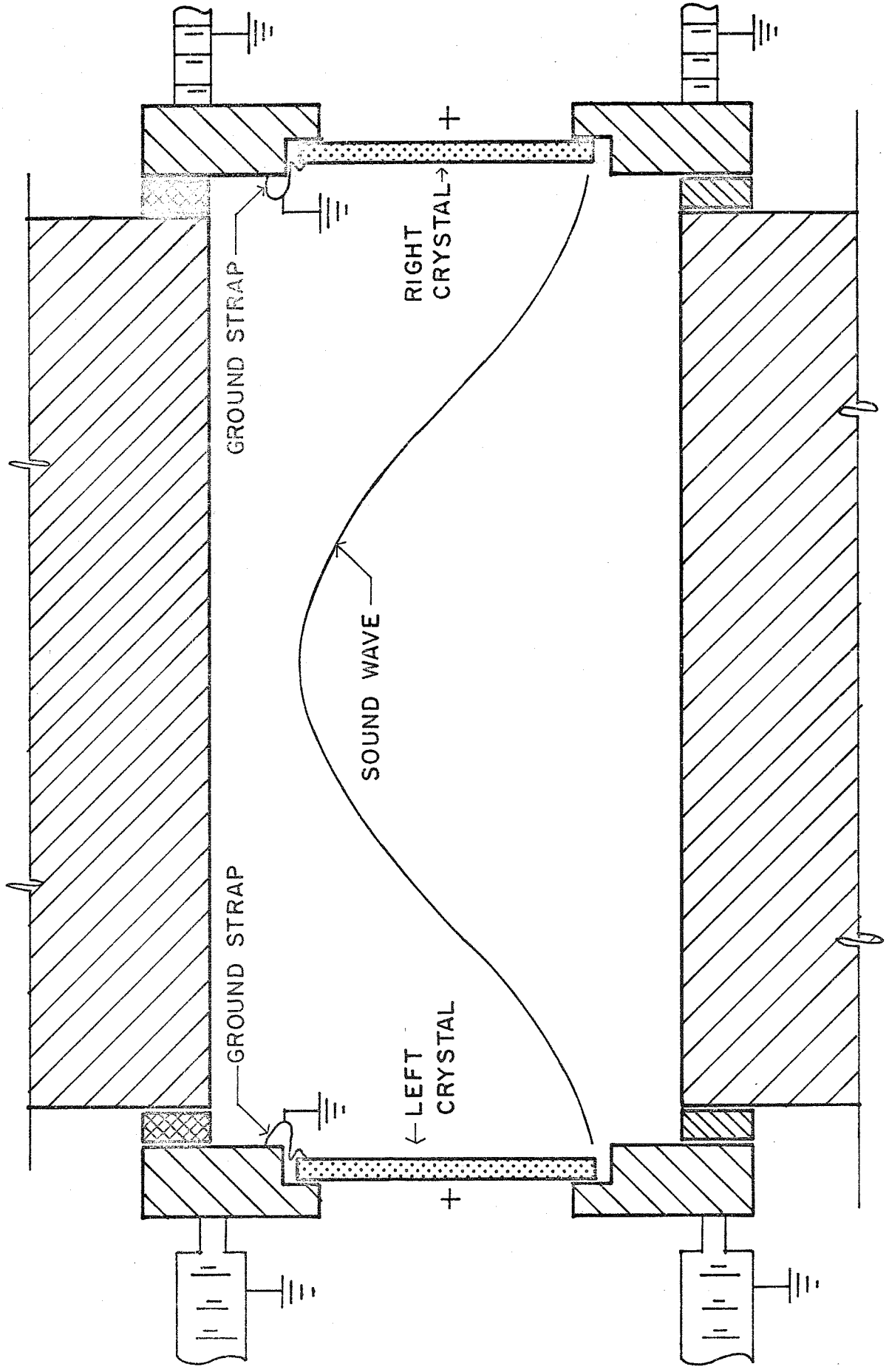

Figure 9 The Resonator Electrical System

at the face in contact with the liquid medium. In a previous report, a continuous ground strap, held in place and grounded to the center of the cavity by the pressure of the rubber O-ring was employed. In the present cell, each crystal is grounded directly to the brass mounting ring using a 0.0625 in. copper strap, and the ring in turn is grounded to the cell housing via the adjustment screws. In this way, it was hoped that possible scattering of the acoustic waves from a continuous strap protruding into the acoustic field and the concomitant reduction in sensitivity would be avoided.

A sinusoidal voltage is impressed across the left crystal via the center conductor of a BNC connector. The piezoelectric transducer responds to the driving voltage by vibrating in its thickness mode at the driving frequency. The face in contact with the specimen liquid thus produces an acoustic disturbance which propagates according to its acoustical properties. The sound wave striking the left face of the right crystal produces a mechanical disturbance in this transducer which results in a voltage appearing at its terminals, which is fed to the external circuitry via the BNC connector and copper strap extending over its right face.

Figure 10 is a block diagram of the electronic instrumentation. The continuous wave signal is provided by a Ferris, Model 22-A Standard Signal Generator having a frequency range of 85 kHz to 25 MHz and a maximum signal output of 1 volt. The driver (input) signal is amplified and fed to a Systron Donner Frequency Counter model 1037. The received signal at the right transducer is amplified by a cascaded bank of three Hewlett Packard Model 460A variable gain (0 - 20 db) Wide Band Amplifiers and one Hewlett Packard Model 461A (40 db) Wide Bank Amplifier. The 80 db of

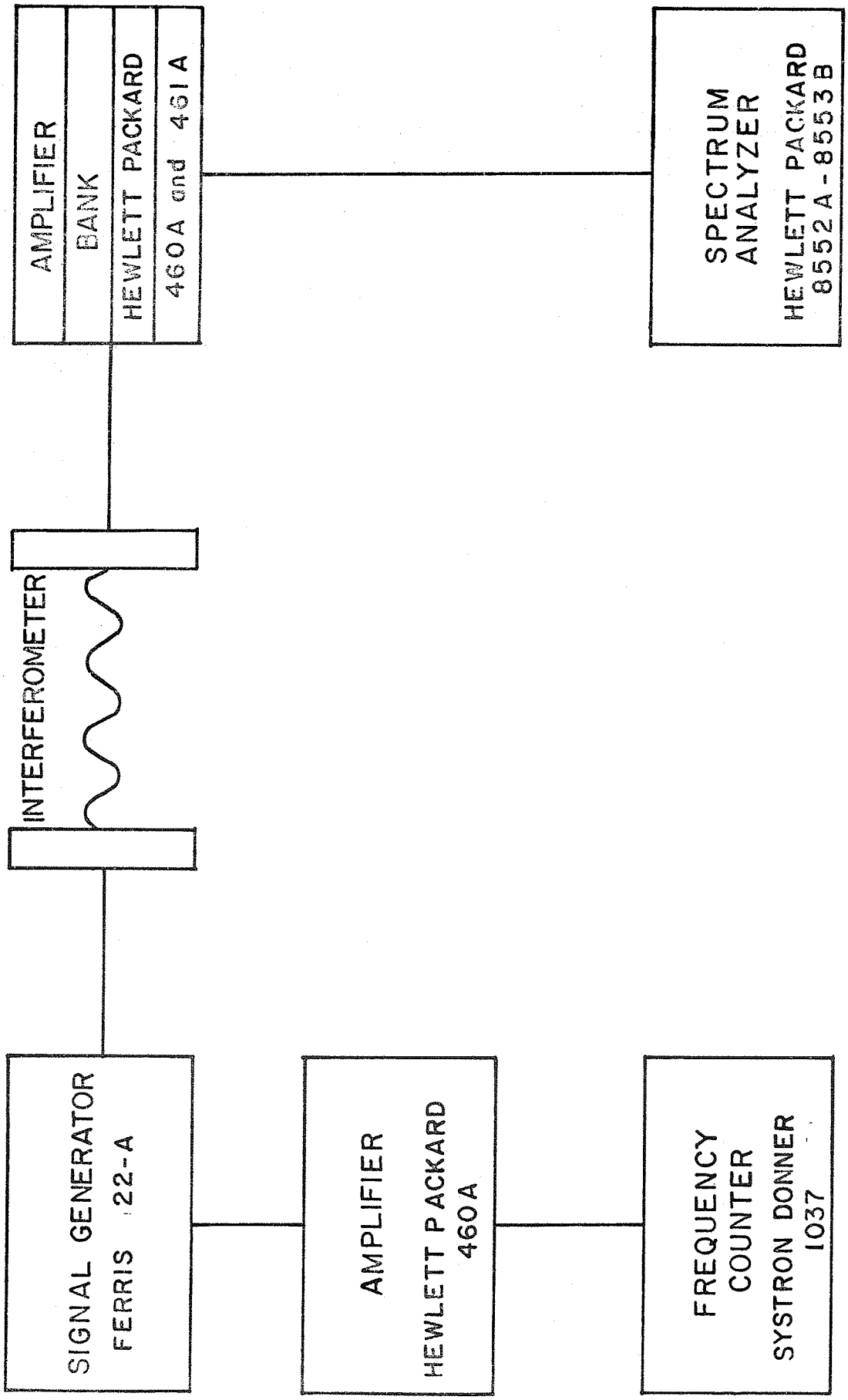

Figure 10 The Electronic Instrumentation

achievable gain was particularly necessary at frequencies near the even harmonics of the crystals. Near the resonance frequencies, where the signal is strong, the gain must be reduced to avoid nonlinear amplification. After amplification, the signal was fed into a Hewlet Packard Model 8552A-8553B spectrum analyzer.

IV. MEASUREMENT PROCEDURE

A. Charging the Cell

Figure 11 is a photograph of the cell, prepared for charging. The cell and all of its components must be cleansed thoroughly prior to charging with the liquid specimen. Water and acetone rinses were used. The charging of the cell must be accomplished without introduction of air bubbles which scatter sound waves and otherwise alter the acoustic propagation properties of the media, resulting in a decreased Q.[5] The charging procedure begins with the closing of the wing valve, assembling the receiver side of the cell, and then resting the cell on the receiver end with the transducer facing upward. The specimen fluid is then slowly added from the unassembled sending portion of the cell with a syringe and hypodermic needle in such a manner that gas bubbles are not formed in the various crevasses, such as under the ground strap. However, air frequently appeared trapped around the rubber O-ring and had to be jarred loose with a needle.

The sending crystal, gasket, and all remaining structures are then assembled to the unit, and the cell is uprighted and returned to its wooden cradle. At this stage, about 6 ml of the specimen fluid must still be added through the loading tube. The valve on the tube is opened to allow fluid in the cavity to fill the tube, before the syringe is inserted, to prevent the air in the tube from being forced into the cavity. Fluid necessary to fill completely the cavity is then introduced from the bottom of the cell. Examination verified that loading in this manner, compared to loading the cell completely through the tube, greatly reduced trapped gas bubbles. Care

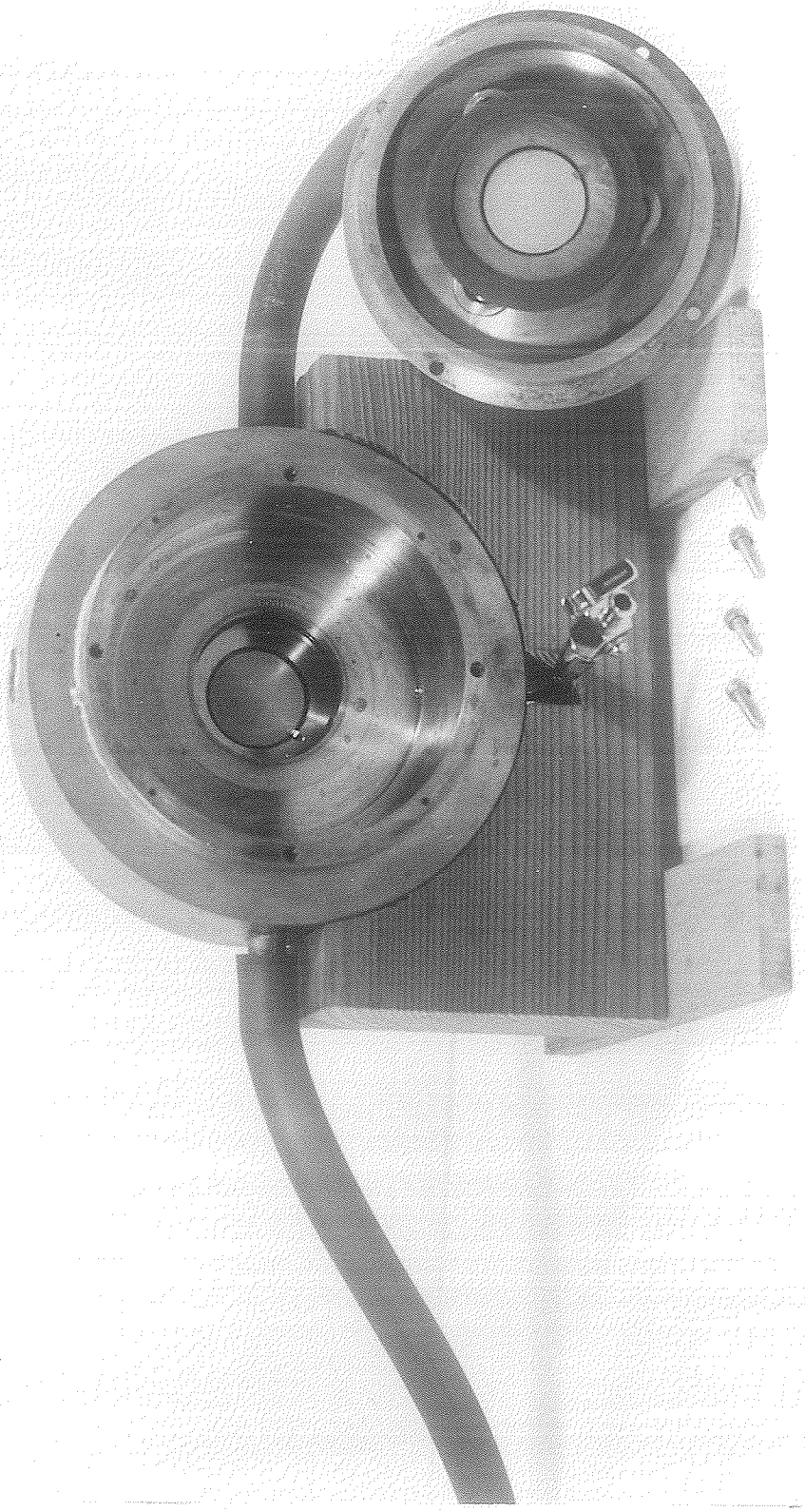

Figure 11 Photograph of Partially Dismantled Cell

must also be taken not to allow the vaseline, used to seal the gaskets, to contaminate the specimen liquid.

B. Crystal Alignment

Perfect parallelism between the two quartz crystal transducers is assumed in the development of the theory governing the operation of the cell and is therefore essential if accurate measurements are to be obtained. Alternatively, the importance of crystal parallelism can be seen by estimating the time it takes for the acoustic pressure wave to decay to 37 percent of its original amplitude, sometimes called the "average life span of the phenomenon, T."[3]

$$T = \frac{Q}{2\pi f_n} = \frac{1}{2\pi \Delta f} \tag{40}$$

For a typical half-power band-width of Δf = 200 Hz at 2 MHz in water, T is about 8×10^{-4} sec. This corresponds to a sound path in the resonator of about 1.2 meters. For the present case where the cavity length is 18 mm, T represents approximately 67 reflections. Thus, in order to avoid effects arising from diffraction phenomena, the crystal alignment procedure is of great importance.

Figure 12 is an oscilloscope display of the magnitude of the acoustic wave amplitude in the cell versus frequency when the unit is excited by a constant voltage swept signal from a General Radio Standard Sweep Frequency Generator Type 1025-A. The frequency range shown in the figure is about 0.4 MHz, and the peak of greatest magnitude occurs at the fundamental

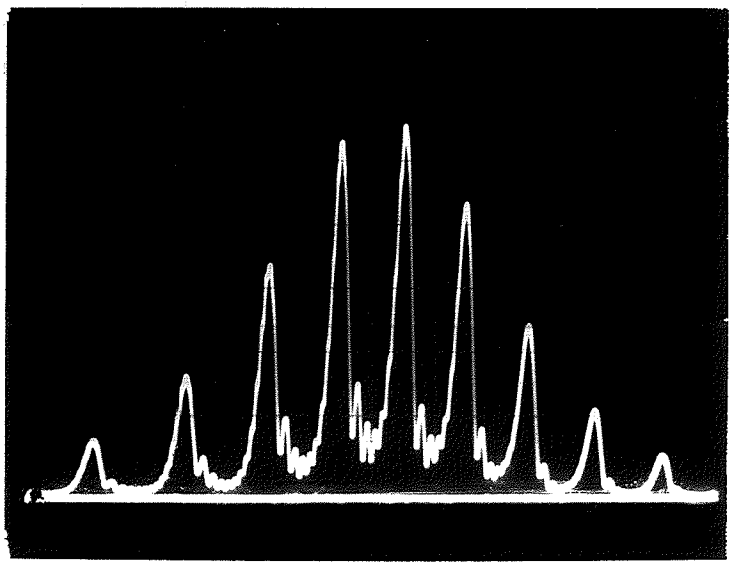

Figure 12 Frequency Response

frequency of the crystals, viz., 2.206 MHz. The exciting voltage is 0.9 Volt RMS, and the output is shown on a scale of 0.5 V/division. The sweep rate is too fast to exhibit the smooth, steady-state response of the resonance peaks. The figure does show nine resonance peaks upon which adsorption and velocity information depend.

Initial adjustment of the quartz crystal transducers is carried out with the sweep generator. The large sending end and the small receiving end screws are manipulated to increase the size of the resonance peaks shown in Fig. 12. When the output cannot be perceptibly improved, the spectrum analyzer is used for more precise alignment. The output signal of the receiver transducer is a sinusoid of the same frequency as the input signal

to the transmitter transducer. This output signal is fed into the spectrum analyser, and a Fourier Analyses of the signal is displayed in the form of a single spike. When the signal generator frequency, which drives the transmitter transducer, is increased from a frequency below one of the resonance frequencies to a frequency above the resonance frequency, the tip of the analyser spike traces out the shape of the resonance, curve as illustrated in Fig. 13. The resonator under investigation was most effective in the frequency range of 3 to 24 MHz and a resonance near the center of this range, viz., around 12 MHz, was used for tuning. It occurred that when other frequencies, nearer to the ends of this frequency range, were used for tuning, the cell was less likely to be tuned for the entire range of frequencies to be covered.

The alignment procedure is as follows: The signal generator is set to the center frequency of the resonance curve to be used, i.e., to the frequency where the analyser spike amplitude is greatest. The crystals are then adjusted in a trial and error process with the goal of the alignment procedure being to produce as sharp a resonance curve as possible. Initially, the receiving end adjustment screws are used to maximize the analyser amplitude. When no further improvement is achieved with these screws, the fine screws on the sending side are used. While no established procedure for adjusting these screws was developed, clockwise sequence for adjustment seemed appropriate and convenient. During the period when these adjustments were being made, the signal generator had to be observed to insure that it had not drifted from the chosen center frequency. At this stage in the development of the unit, proper adjustment can only be ascertained by comparing a measured value of acoustic absorption or velocity

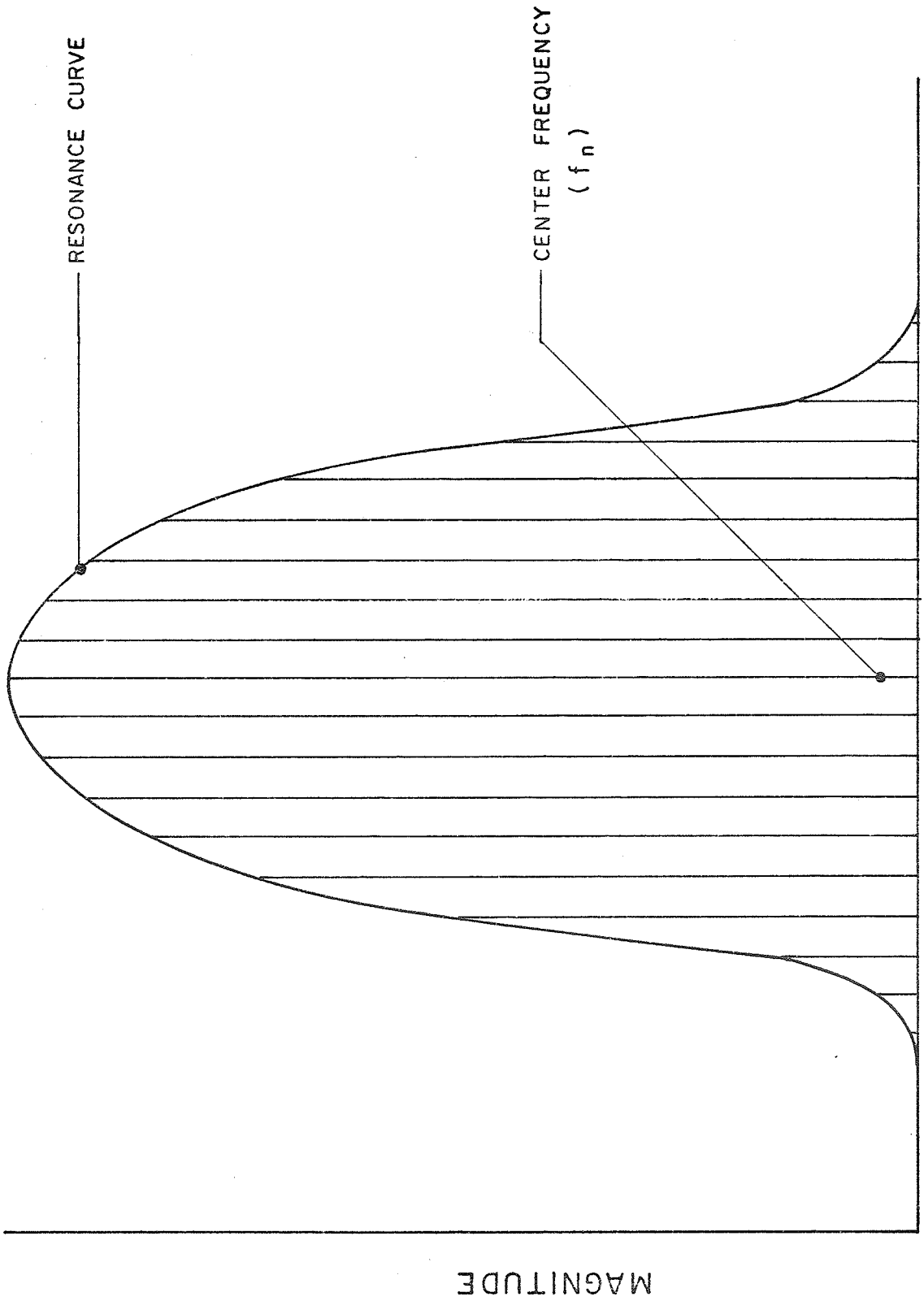

Figure 13 Output Magnitude Versus Frequency

with accepted values.

C. The Absorption Measurement

As shown in Sec. II.C, the absorption per wavelength ($\alpha\lambda$) value depends upon the bandwidth of the resonance peak and the procedure for its determination is as follows. The cell is thoroughly cleansed, dried, and charged with the solution as described in Sec. IV.A; the electrical attachments are made and the transducers are aligned. The signal generator is set at a selected center frequency. The analyser output spike is adjusted, using the spectrum analyser attenuators, until its magnitude is exactly eight divisions on the analyser display screen, and the center frequency, f_n, is recorded. The generator frequency is then increased until the output spike amplitude decreases to half power above resonance, i.e., to a value of 5.66 divisions on the display screen. A permanent marker was installed on the spectrum analyser screen at 5.66 divisions to facilitate the location of the half power points. After the frequency of the half power point is recorded, a similar procedure is followed to locate the half power frequency below resonance. The difference between these two frequencies is the bandwidth, Δf.

Bandwidth measurements are conveniently made every 1 to 2 MHz, beginning with the upper limit of the signal generator (25 MHz) and working toward lower frequencies. At frequencies near the fundamental of the crystals (2.206 MHz) or the odd harmonics, the transducer resonances greatly overpower the resonance of the cell. At the transducers' even harmonics there is no crystal motion, and, therefore, no output signal. These two phenomenon

mean that the data cannot be obtained in bands near the even and odd harmonics of the transducers, and operation is restricted to bands between them. After the data is obtained, the specimen is drained into a pyrex beaker, and any necessary physical and chemical determinations, e.g., concentration of dissolved solutes, are conducted.

Following the measurements with a solution, the left side of the cell is disassembled and the cavity and crystals again thoroughly cleansed and dried. During dismantling and cleansing, neither set of adjustment screws are altered, simplifying the ensuing alignment for the solvent which is to examined. The interferometer is then charged with the solvent and the alignment checked. Bandwidth measurements for the solvent are made at thw resonance peaks closest in frequency to the peaks used for the solution. The solvent and solution resonant peaks do not occur at the same frequency, but may differ by as much as 20 kHz.

After measuring the bandwidths for the solvent, the following equation is applied to complete the measurement.

$$\alpha\lambda_{chemical} = \frac{\pi(\Delta f_{solution} - \Delta f_{solvent})}{f_n} \qquad (41)$$

where f_n is the center frequency of the solution resonance peak.

D. Velocity Measurement

As discussed earlier, the velocity of sound in the solution depends upon the distance between the transducers and the frequency difference between adjacent resonant peaks or resonant center frequencies. The frequency difference is found by recording, from the frequency counter adjacent frequencies producing maximum output spikes on the spectrum analyser and then subtracting,

i.e., forming $f_{n+1} - f_n$.

The design of the cell facilitates measurement of the transducer path length. The procedure is as follows: The receiver side outer brass piece is removed, along with the sending side BNC connector. The distance between the two brass faces is measured with a micrometer yielding a length D. Next, the distance to the outer faces of the two transducers is measured using a depth gauge. The measurement to the sending crystal is made through the hole housing the BNC connector and yields the length D_1. The distance to the receiver crystal is made through the large opening exposed by removal of the outer receiver brass piece and yields a length D_2. The transducer thicknesses T_1 and T_2 are measured prior to assembling the cell and are, of course, constant. The acoustic path length, L, is then found by applying the following relationship (see Fig. 14).

$$L = D - (D_1 + D_2 + T_1 + T_2) \tag{42}$$

Finally, acoustic velocity is computed from

$$C = 2L\,(f_{n+1} - f_n) \tag{43}$$

The acoustic path length measurement is made with the two BNC connectors removed. The contacts extending from these connectors exert slight pressure on the crystal faces, but depth gauge measurements, performed both with and without the presence of the contacts, showed that this pressure produces a change of less than 0.1 percent in determining the value of L.

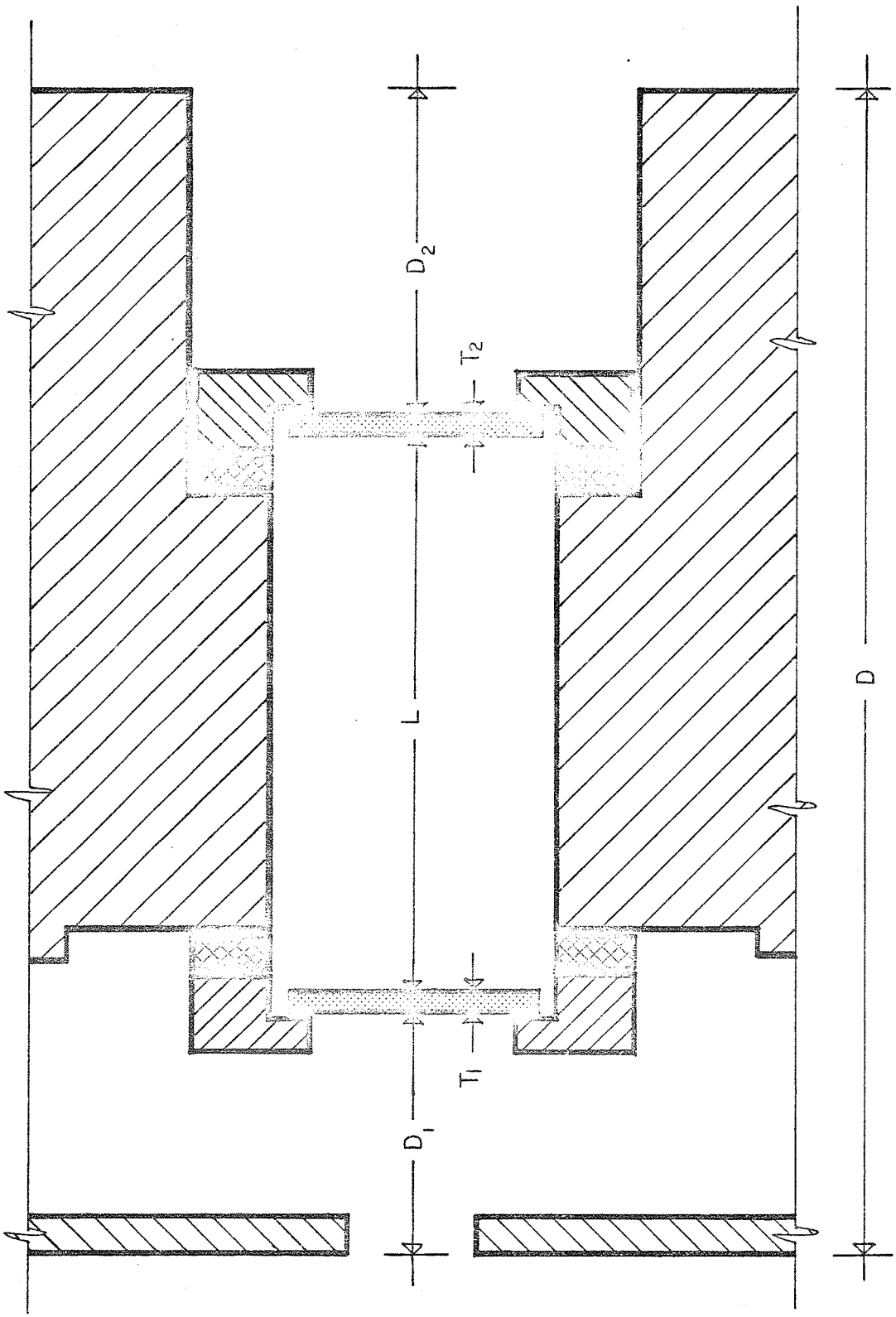

Figure 14 Acoustic Path Length Measurement

V. DISCUSSION OF CELL PERFORMANCE

The interferometer was initially examined using distilled water as the specimen fluid since values of the pertinent acoustic parameters are well known. From the bandwidth relation, Eq. 37, one easily obtains

$$\Delta f = \left(\frac{\alpha}{f^2}\right) \frac{C}{\pi} \times f^2 \tag{44}$$

where $\frac{\alpha}{f^2}$ is the acoustic frequency free absorption coefficent and has the value of $25.0 \times 10^{-15} \frac{sec^2}{m}$ at 20.0°C. The velocity of sound in distilled water at 20°C is 1480 m/sec. Equation 44 suggests the log-log plot as a convenient manner for presenting the data. For a quadradic dependence of the frequency free absorption coefficient with frequency, the bandwidth should appear a straight line of slope 2. Figure 15 is an example of an early set of data showing that the predictions of Eq. 44 are not fulfilled below about 20 MHz. It is recognized that the cell will perform with less accuracy in lower frequency ranges where spreading of the sound beam due to diffraction phenomena is more pronounced.

Substantial improvement was obtained over that of Fig. 15 by making the following alternations:

1. The receiving crystal was mounted as shown in Fig. 7 to allow positioning for parallelism,
2. Quartz plates much more closely matched in frequency were employed (matched to 10 Hz), and
3. Initial mechanical adjustments were made using a swept frequency display rather than a fixed frequency display.

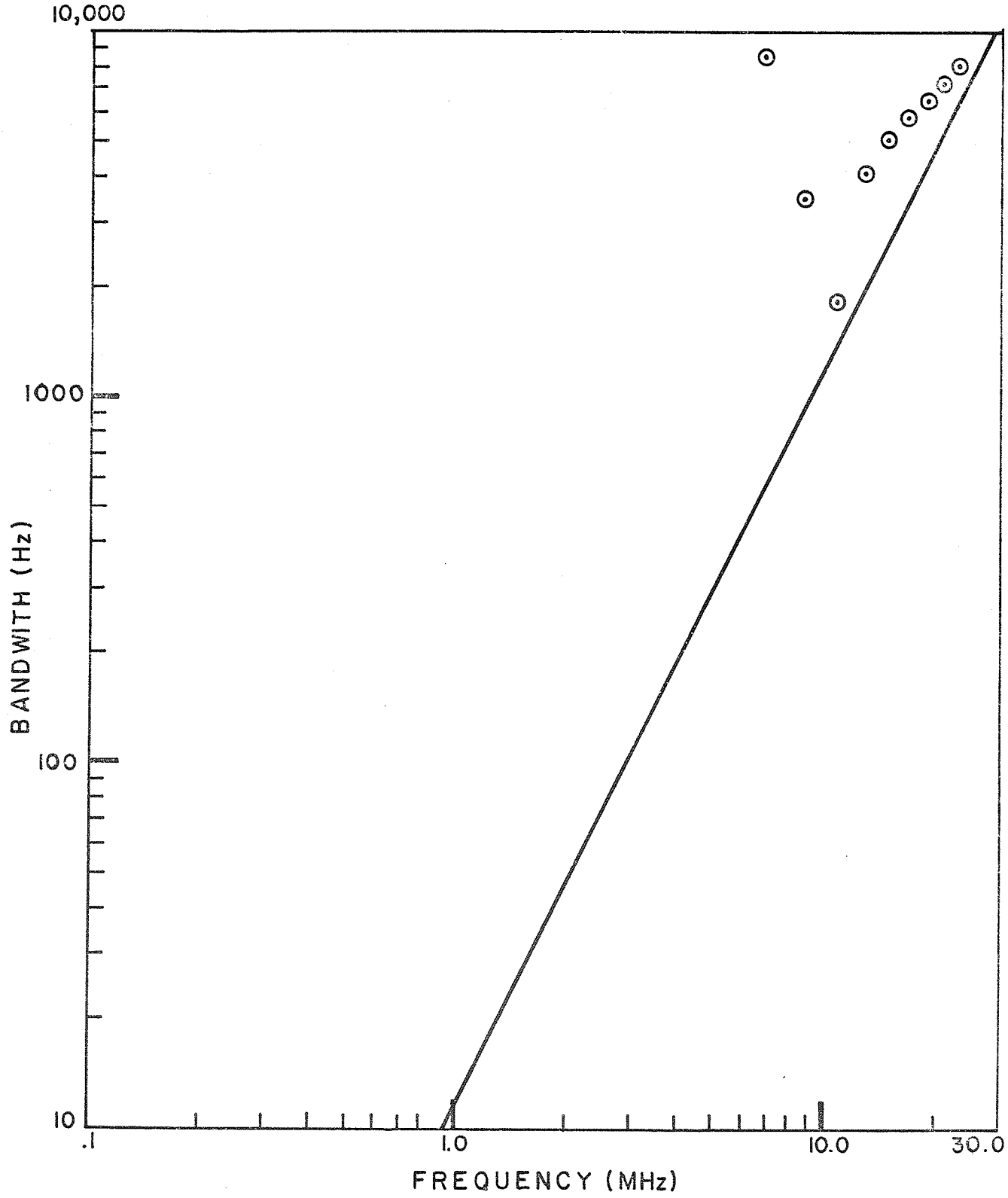

Figure 15 Early Bandwidth Versus Frequency Plot for Distilled H_2O. Straight Line (——) is Equation 46.

Figure 16 shows a typical set of data obtained, after the above alterations were included, together with results obtained by a previous investigation.[3]

An investigation of the speed of sound revealed some significant points regarding the operating characterisitcs of the cell. Figure 17 shows measured sound velocity for distilled H_2O at 20.7°C as a function of frequency in the range 1 to 10 MHz. The transducer fundamental and the third harmonic frequencies are, respectively, 2.206 MHz and 6.618 MHz; the second and fourth harmonics are, respectively, 4.412 MHz and 8.824 MHz. The velocity was determined from Eq. 43. It is apparent in Fig. 17 that measurements must not be made in regions near the fundamental or the odd harmonic frequencies of the transducers and may not be made near the even harmonics. The former are exluded because the high Q of the transducers overpowers the resonance of liquid column and the latter because the received signal is too weak to be processed. Data is obtained at frequencies within bands of from about 1/12 to 2/5 and from 3/5 to 11/12 of the frequency band between adjacent odd harmonics (See Fig. 17, for example). The velocity of sound in distilled H_2O at 20.7°C was determined with an uncertainty of 0.3 percent of the accepted value.

Figure 18 shows the experimentally determined speed of sound in a 10.65 percent solution of polyethylene glycol (PEG) of molecular weight of 20,000, in water. A previously determined value of velocity for a 10.65 percent solution is 1550 m/sec[6] and the present determination is 1557 m/sec, i.e., an uncertainty of 0.5 percent. From Eq. 41 one easily obtains

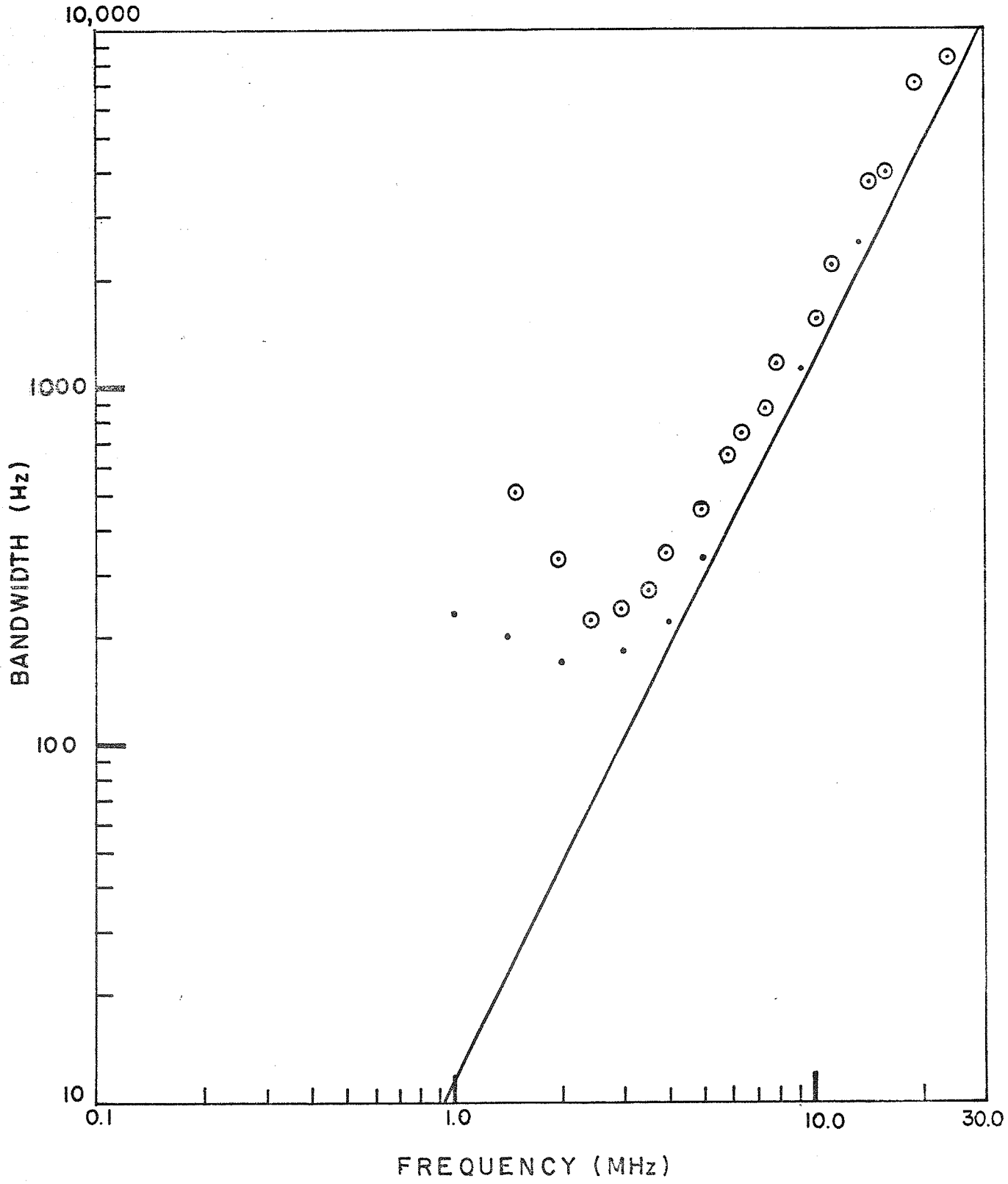

Figure 16 Bandwidth Versus Frequency Plot for Distilled H_2O at 20.7°C. Data from Present Study is Circled (⊙) and Data by F. Eggers is Uncircled (•). Straight Line (——) is Equation 46.

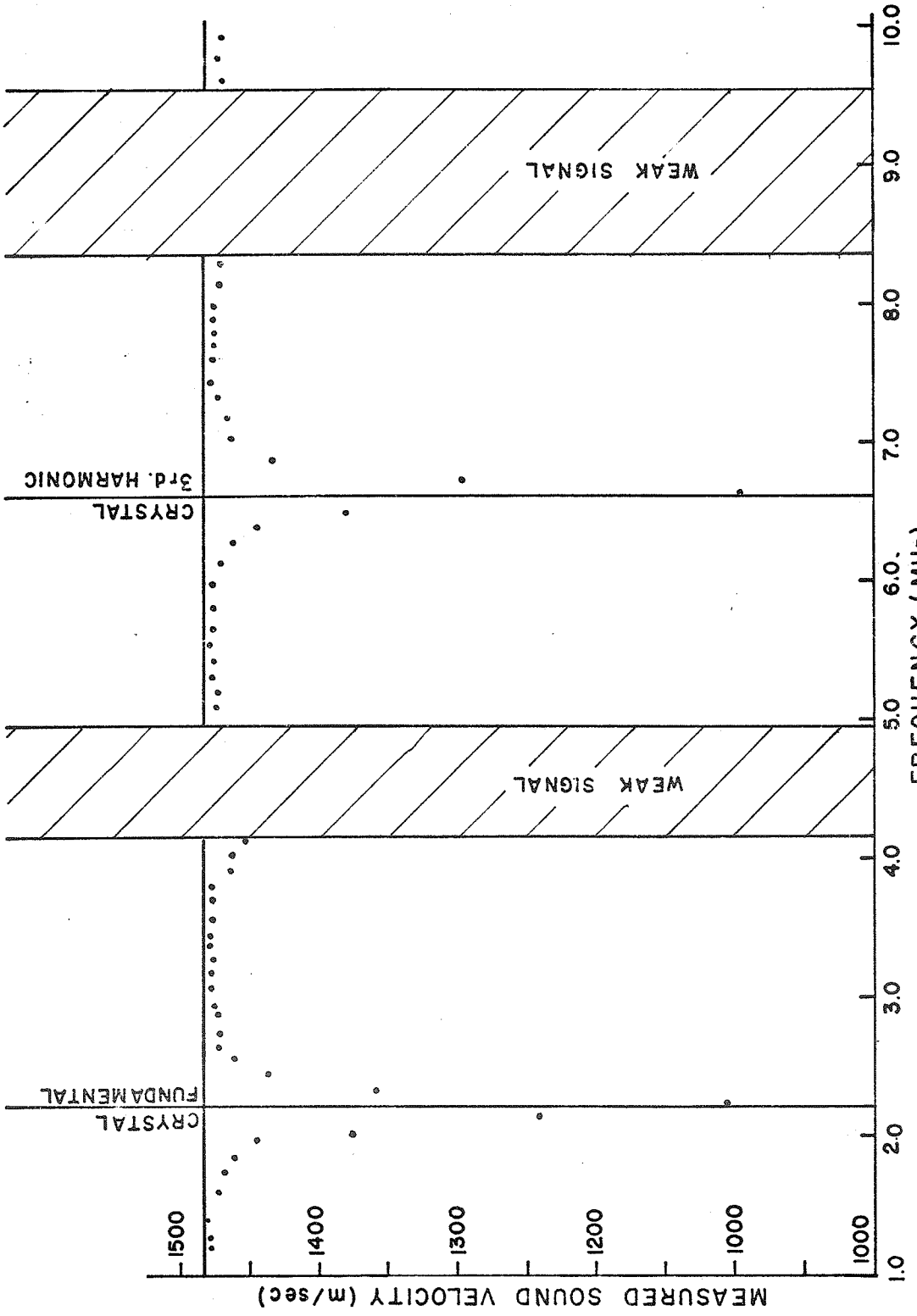

Figure 17 Measured Sound Velocity in Distilled H_2O at 20.7°C Versus Frequency

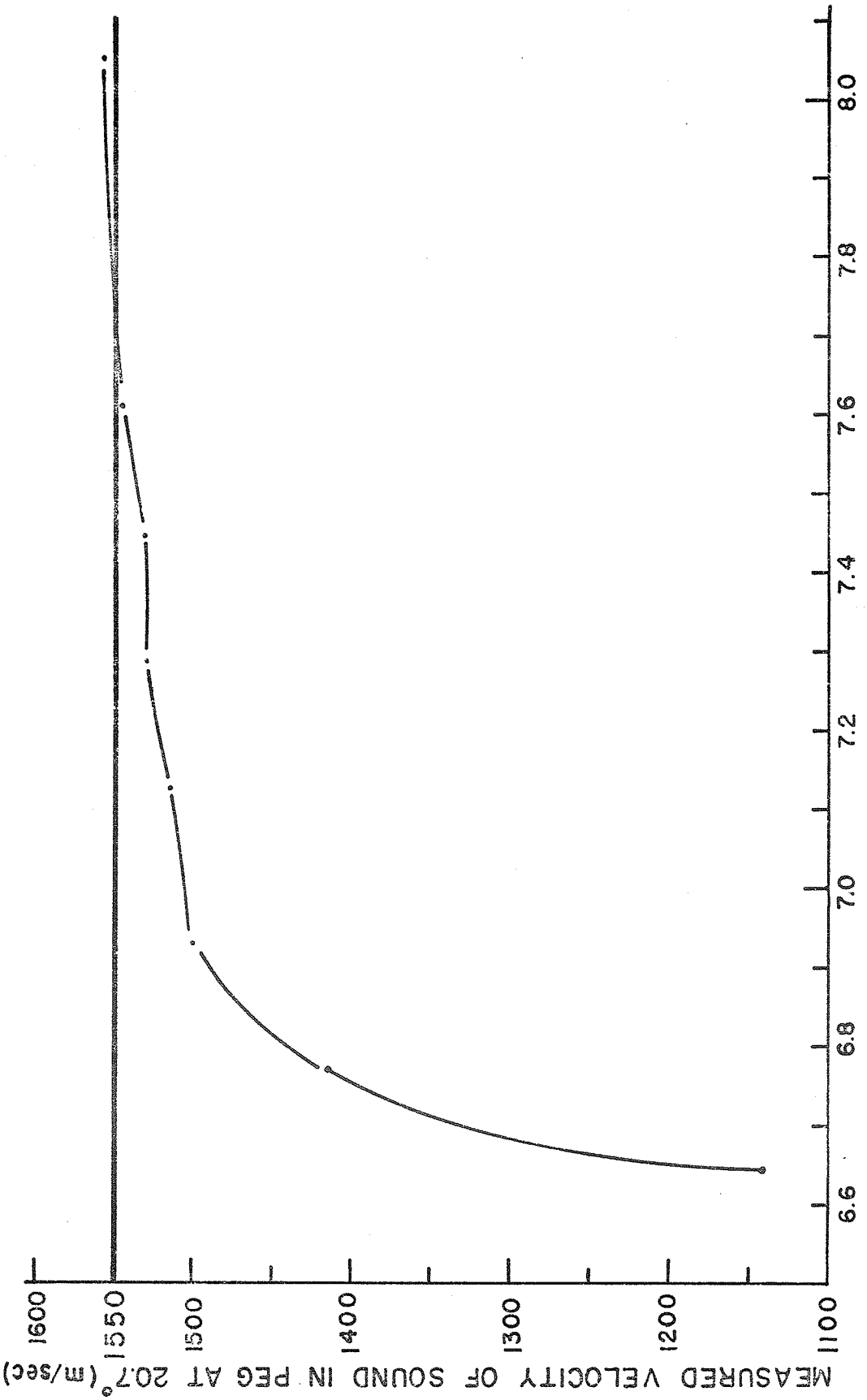

Figure 18 Measured Velocity of Sound in 10.65 Percent Solution of PEG at 20.7°C. Straight Line (——) is Known Value

$$\frac{\alpha}{f^2 conc} = \frac{(\Delta f_{solution} - \Delta f_{H_2O})\ \pi}{(f^2\ C)\ conc} \qquad (45)$$

The frequency free absorption per unit concentration ($\alpha/f^2 conc$) for the above PEG solution was determined using Eq. 45. Figure 19 shows the values from this study together with those from an earlier work.[6]

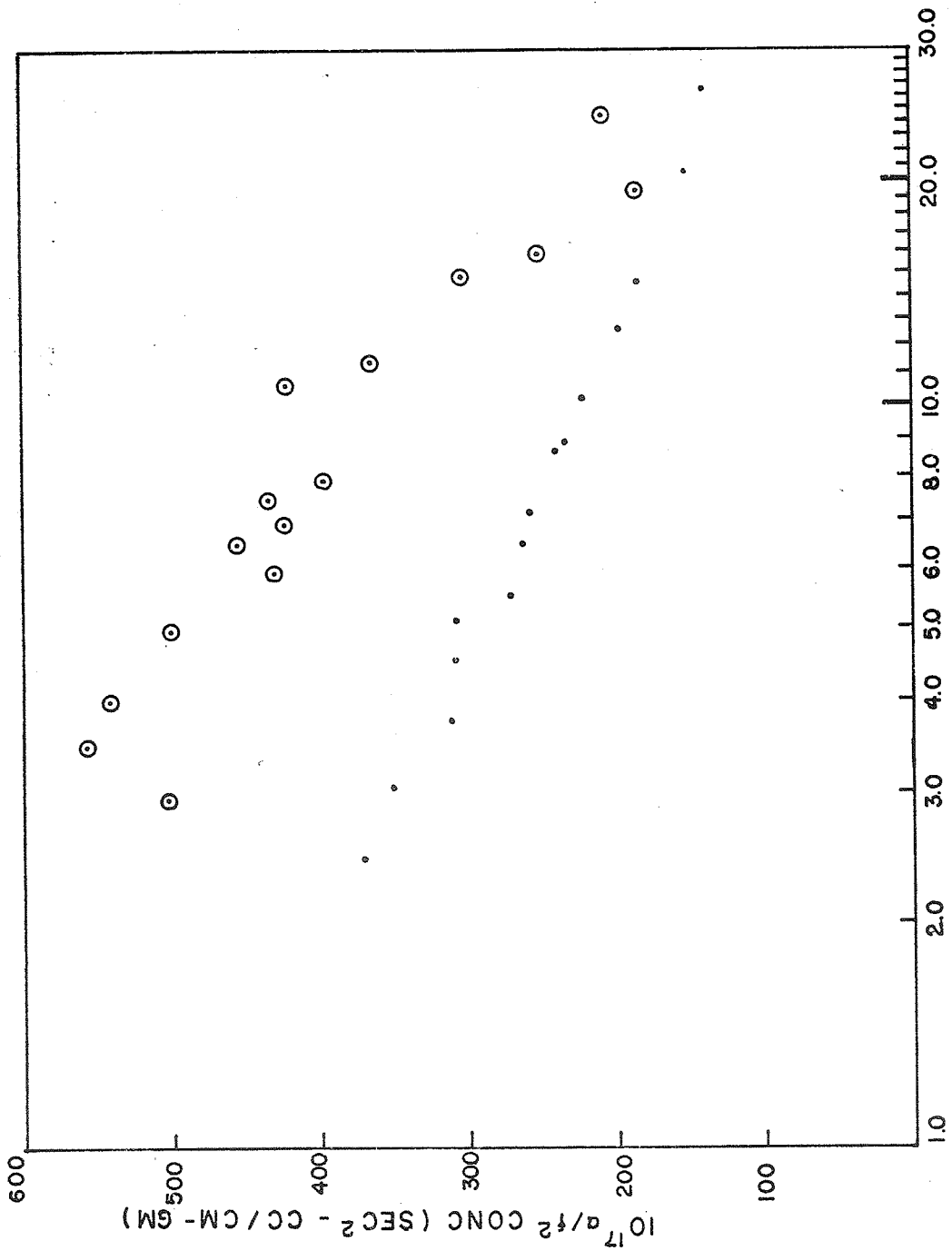

Figure 19 Frequency Free Absorption Per Unit Concentration Versus Frequency at 20.7°C. Data From Present Study is Circled (⊙) and Data by L. Kessler is Uncircled (•).

VI. DISCUSSION OF ERRORS

Two major sources of error are those associated with alignment of the transducers and those associated with the instrumentation procedures.

The interferometer is extremely sensitive to transducer alignment, i.e., slight variations in alignment produce appreciable changes in the Q of the system, with the Q being reduced in magnitude as deviations from true parallelism occur. As an example, Table 1 shows the measured bandwidths for distilled H_2O at 20.7°C at four frequencies. Column A is the bandwidth for what is believed to be near perfect alignment, and Column B is the resulting bandwidth after one of the 3/8-64 screws has been rotated 15°, i.e., a longitudinal displacement of 0.017 mm.

Table 1

Center Frequencies and Bandwidths

Center Frequency	A Near Perfect Alignment Bandwidth	B Misaligned Bandwidth
2.9 MHz	238 Hz	287 Hz
6.00 MHz	717 Hz	2,458 Hz
12.00 MHz	2,593 Hz	6,148 Hz
23.84 MHz	11,921 Hz	20,157 Hz

It must be recalled that the theory of the operation of the unit assumes perfect parallelism of the transducer surfaces and the existence of

plane waves. Thus, deviation from these conditions produces a situation which cannot be interpreted using the available theory. When working with a liquid of unknown acoustic properties, the cell transducer alignment is adjusted for minimum bandwidth after which the data is established. In those special cases where a known reference liquid having a speed of sound nearly identical to that of the unknown is available, the procedure can include aligning the transducers until accepted values are obtained for the known fluid and then, being careful not to alter the alignment, the reference material is removed and replaced by the unknown, which is then measured. Disadvantages of this procedure are associated with the dismantling, cleansing, and drying of the cell after the reference liquid has been treated and the unknown is introduced, which may be sufficiently severe as to affect alignment.

The sources of error associated with the instrumentation and procedure are listed in Table 2.

Table 2

Equipment Error Sources

Frequency Stability during experimental measurement		
a.	< 5 MHz	± 0.025%
b.	> 5 MHz	± 0.001%
Temperature Stability		± 0.1°C
Uncertainty in Temperature Measurement		± 0.2°C
Uncertainty in Acoustic Path Length (L) Measurement		± 0.02 mm
Uncertainty in Concentration of polyethelene Glycol solutions		± 0.1%
Bandwidth Measurement	a. < 5 MHz	± 1.0%
	b. > 5 MHz	± 2.0%

VII. SUMMARY AND FUTURE DIRECTIONS

The following summarizes briefly the contents of this thesis.

1. A two piezoelectric transducer, fixed path interferometer has been constructed to determine speed of sound and by a comparative method, the ultrasonic absorption in small volumes (18 ml) of liquid media.
2. Frequency bands in which useful data can be obtained are related to the fundamental thickness resonant frequency of the closely matched pair of transducers and for the 2.206 MHz plates employed in this study are generally 0.3 MHz to 1.7 MHz on either side of the odd harmonics.
3. The interferometer is capable of providing determination of the velocity of sound with an accuracy of 0.5 percent.
4. Determinations of the acoustic frequency-free absorption coefficient in polyethylene glycol appear to yield values in excess of those generally accepted, and the reasons for this are unknown at this writing.

It is believed that further improvements can produce a practical device. Those identified for immediate study are:

1. The Q of the system must continue to be improved. One possible source of a decrease in Q, at high frequencies, could be ripples along the surface of the transducer, causing oblique reflections. Assuming that a ripple with a lateral dimension of 10 percent of the wave length of the acoustical wave could cause an oblique reflection, then lowering of the

the Q could occur at 20 MHz with a ripple of 0.007 mm in length. Therefore, the crystals should be inspected for optical flatness.[5]

2. The General Radio Company type 1025-A Standard Sweep Frequency Generator used in this study sweeps a frequency range of 1.3 MHz at a rate of 20 sweeps per second. Since the bandwidths in the lower frequency range are only several hundred Hz, the system is being swept too fast to respond with a steady state output. In order to observe the steady state frequency response of a single resonance during the alignment procedure, a device should be obtained that would sweep a smaller frequency band, on the order of 1 kHz.
3. For the case where alignment of the transducers is carried out with a reference fluid and the unknown is introduced after dismantling, cleansing, and drying, a different design should be considered to minimize the opportunity for severe treatment leading to inadvertant misalignment. One method suggested involves cutting the cell in such a way that dismantling would open the cell along a plane midway through the cavity, instead of opening at the ends as is done in the present model.
4. The current model was fabricated of brass because of ease of machining and availability. Future models should be fabricated of materials less chemically active in order to provide more versatility as regards chemically active materials to be studied.

LIST OF REFERENCES

1. Macleod, R. M., Dunn, F., J. Acoust. Soc. Am., 44, 1968, p. 932.

2. McSkimin, H. J., Physical Acoustics, Vol. 1, Part A, Chapter 4, Academic Press, New York, 1964, p. 272.

3. Eggers, F., Acustica, 19, 1968, p. 323.

4. Kinsler, L. E., and Frey, A. J., Fundamentals of Acoustics, John Wiley & Son, New York, 1962, p. 196.

5. Eggers, F., Private Communication.

6. Kessler, L. W., O'Brien, W. D., Jr., Dunn, F., J. Phys. Chem., 74, 1970, p. 4096.